Cancer Management and Research

Dovepress

open access to scientific and medical research

Open Access Full Text Article

ORIGINAL RESEARCH

Downregulation of circRNA_0000285 Suppresses Cervical Cancer Development by Regulating miR197-3p–ELK1 Axis

This article was published in the following Dove Press journal:
Cancer Management and Research

Wenmin Zhang[1]
Suping Zhang[2]

[1]Department of Obstetrics and Gynecology, Heze Municipal Hospital, Heze, Shandong 274000, People's Republic of China; [2]Department of Reproductive, Zoucheng People's Hospital, Zoucheng, Shandong 273500, People's Republic of China

Background: Circular RNAs (circRNAs) are involved in the development of human cancers, including cervical cancer (CC). However, the role and mechanism of the circRNA *hsa_circ_0000285* (*circ_0000285*) in CC development remain largely unknown.

Methods: Thirty paired CC and adjacent normal tissue samples were harvested. CC cell lines SiHa and HeLa were cultured in this study. The expression of *circ_0000285*, *miR197-3p* and *ELK1* was detected via qRT-PCR or Western blot. CC development was assessed via cell viability, colony formation, apoptosis, cell cycle, and autophagy using MTT, colony-formation assays, flow cytometry and Western blot. The target association was analyzed via dual luciferase–reporter assay, RNA immunoprecipitation, and RNA pull-down. The role of *circ_0000285* in CC in vivo was analyzed using a xenograft model.

Results: *circ_0000285* abundance was enhanced in CC tissue and cells and mainly located in cytoplasm. Silence of *circ_0000285* suppressed cell viability and colony formation, arrested the cell cycle at the G_0/G_1 phase, and induced apoptosis and autophagy in CC cells. *miR197-3p* was targeted by *circ_0000285*, and *miR197-3p* knockdown reversed the effect of *circ_0000285* silence on CC development. *miR197-3p* directly targeted *ELK1* to inhibit CC development. *circ_0000285* regulated *ELK1* by modulating *miR197-3p*. Knockdown of *circ_0000285* reduced xenograft tumor growth in vivo.

Conclusion: Knockdown of *circ_0000285* repressed CC development by increasing *miR197-3p* and decreasing *ELK1*.

Keywords: cervical cancer, *circ_0000285*, *miR197-3p*, *ELK1*

Introduction

Cervical cancer (CC) is a common disorder of female reproductive system, including squamous-cell carcinoma and adenocarcinoma.[1] It is one of the leading causes of cancer-related death in females, with high incidence and mortality worldwide.[2] Current options for CC treatment have made considerable advances, while outcomes for CC patients at the advanced stage remain poor.[3] As such, new insights into the pathogenesis and treatment of CC are urgently needed.

Recently, a study focused on the role of circular RNAs (circRNAs) in gynecological diseases, including CC.[4] circRNAs are a group of noncoding RNAs produced via covalently closed loops through back-splicing with a lack of polyadenylation and capping.[5] circRNAs play important roles in the development, diagnosis, prognosis, and treatment of human cancers.[6] They may regulate miRNAs and their targeted genes through the competing endogenous RNA (ceRNA)

Correspondence: Suping Zhang
Tel +86-537-6626135
Email ofwnvx@163.com

submit your manuscript | www.dovepress.com
DovePress
http://doi.org/10.2147/CMAR.S253174

network.[7] Moreover, dysregulated circRNAs are implicated in the carcinogenesis and development of CC.[8] *hsa_circ_0000285* (*circ_0000285*) is a circRNA derived from *HIPK3*, which has an important role in CC development.[9] Studies have indicated that *circ_0000285* takes part in malignancies of multiple cancers, including nasopharyngeal carcinoma, bladder cancer, osteosarcoma, and laryngocarcinoma.[10,13] More importantly, emerging evidence suggests that *circ_0000285* promotes proliferation and metastasis of CC.[14] Although dysregulated *circ_0000285* is involved in CC, how *circ_0000285* regulates CC development is largely unclear.

miRNAs are noncoding RNA molecules with 19–25 nucleotides that exhibit key roles in the development and treatment of CC.[15] *miR197-3p* has been suggested to participate in cancer development via serving as an oncogene or tumor suppressor.[16,17] Moreover, *miR197-3p* can suppress proliferation and invasion of CC cells.[18] However, whether *miR197-3p* is required for *circ_0000285*-mediated regulation of CC development is unclear. Furthermore, *ELK1* has been suggested to have a carcinogenic role in human cancers, like breast cancer, thyroid cancer, hepatocellular carcinoma, and colorectal cancer.[19,22] Emerging evidence has indicated that *ELK1* could serve as an oncogene in CC via promoting cancer development.[23,24] Here, we found there might be ceRNA cross talk of *circ_0000285–miR197-3p–ELK1* because of the potential complementary sequence between them predicted via Circular RNA Interactome and StarBase tools. In this research, we measured *circ_0000285* expression in CC and explored the effect of *circ_0000285* on CC development in vitro and in vivo. Moreover, we explored the ceRNA network of *circ_0000285–miR197-3p–ELK1* in CC cells.

Methods

Patient Tissue

Thirty CC patients were recruited from Zoucheng People's Hospital. Tumor-tissue and paired adjacent normal-tissue samples were obtained via surgery and stored at −80°C until use. The patients did not receive other therapy before tissue collection. The clinical features of patients are shown in Table 1. All patients provided written informed consent. This study was permitted via the Ethics Committee of Zoucheng People's Hospital.

Cell Culture

Human CC cell lines (SiHa and HeLa) and normal cervical epithelial cells (H8) were obtained from BeNa Culture Collection (Beijing, China). DMEM (HyClone, Logan, UT, USA) was used for SiHa cells and RPMI 1640 medium (Thermo Fisher Scientific, Waltham, MA, USA) for HeLa and H8 cells. All cells were maintained at 37°C and 5% CO_2 in complete medium with 10% FBS and 1% antibiotic (Thermo Fisher Scientific).

Table 1 Associations between *circ_0000285* expression and clinical features of CC patients

Clinical Features	n	*circ_0000285* expression		*P*-value
		Low (n=15)	High (n=15)	
Age (years)				*P*>0.05
<45	12	5	7	
≥45	18	10	8	
Tumor size (cm)				*P*<0.05
<4	16	10	6	
≥4	14	5	9	
Differentiation				*P*<0.05
Good/moderate	17	11	6	
Poor	13	4	9	
FIGO stage				*P*<0.05
I	20	12	8	
II	10	3	7	
Lymph-node metastasis				*P*>0.05
Yes	12	5	7	
No	18	10	8	

Abbreviation: FIGO, International Federation of Gynecology and Obstetrics.

RNA Extraction and Quantitative Reverse-Transcription Polymerase Chain Reaction

RNA was isolated with Trizol (Sigma-Aldrich, St Louis, MO, USA). Nuclear and cytoplasmic RNA was extracted with a Paris kit (Thermo Fisher Scientific) according to the manufacturer's instructions. For circRNA extraction, RNA was further incubated with RNase R (GeneSeed, Guangzhou, China) at 37°C. RNA was reverse-transcribed to cDNA using a specific reverse-transcription kit (Thermo Fisher Scientific). cDNA was mixed with SYBR Green (Thermo Fisher Scientific) and specific primers, then applied to qRT-PCR on an ABI 7900 system (Foster City, CA, USA). Primers were generated from Sangon (Shanghai, China): *circ_0000285* (sense, 5′-TACCTCTGCAGGCAGGAACT-3′; antisense, 5′-TCACATGAATTTAGGTGGGACTT-3′),

linear_0000285 (sense, 5′-TGGATATTTGTAAGTCCCACCT-3′; antisense, 5′-TGTGGTCAATGCCTGACTTC-3′), *ELK1* (sense, 5′-TCAACTTTCAGGAGACCCGT-3′; antisense, 5′-TGGCATGGTGGAGGTAACAG-3′), *miR197-3p* (sense, 5′-ACACTCCAGCTGGGTTCACCACCTTCTCCA-3′; antisense, 5′-TCGTGGAGTCGGCAATTCAGTTGAGGCT-3′), *U6* (sense, 5′-CTCGCTTCGGCAGCACA-3′; antisense, 5′-AACGCTTCACGAATTTGCGT-3′), and *GAPDH* (sense, 5′-CTCTGCTCCTCCTGTTCGAC-3′; antisense, 5′-AAATGAGCCCCAGCCTTCTC-3′). *GAPDH* (for *circ_0000285*, *linear_0000285*, *ELK1*, or cytoplasm) and *U6* (for *miR197-3p* or nuclear RNA) served as internal controls. Relative RNA expression was determined by the $2^{-\Delta\Delta Ct}$ method.[25]

Cell Transfection

A *circ_0000285*-overexpression vector was constructed using a pCD5-ciR vector (GeneSeed), with a pCD5-ciR vector alone as negative control (NC; vector). An *ELK1*-overexpression vector (pc-ELK1) was constructed using a pcDNA3.1 vector (Thermo Fisher Scientific). The empty pcDNA3.1 vector was exploited as NC (pc-NC). siRNA for *circ_0000285* (si-circ_0000285, 5′-CCCCAGCUAUUCAAGUGUAAA-3′), siRNA NC (si-NC; 5′-AAGACAUUGUGUGUCCGCCTT-3′), *miR197-3p* mimic (5′-UUCACCACCUUCUCCACCCAGC-3′), miRNA NC (miRNA NC, 5′-CGAUCGCAUCAGCAUCGAUUGC-3′), *miR197-3p* inhibitor (5′-GCUGGGUGGAGAAGGUGGUGAA-3′), and inhibitor NC (5′-CUAACGCAUGCACAGUCGUACG-3′) were synthesized via GenePharma (Shanghai, China). CC cells were transfected with the constructed vectors (600 ng) or oligonucleotides (40 nM) using Lipofectamine 3000 reagent (Thermo Fisher Scientific) for 24 hours.

MTT and Colony-Formation Analysis

Cell viability was assessed via MTT assays. SiHa and HeLa cells (10^4 cells/well) were added to 96-well plates and incubated for 48 hours. At the end point, MTT (Beyotime, Shanghai, China) at a final concentration of 0.5 mg/mL was injected and cells maintained for 4 hours. Next, the medium was changed to 200 μL dimethyl sulfoxide (Beyotime). Absorbance at 570 nm was examined with a microplate reader (Bio-Gene Technology, Guangzhou, China). For colony-formation assays, SiHa and HeLa cells (500 cells/well) were added to six-well plates and incubated for 10 days. The colonies were mixed with methanol (Sigma-Aldrich) and stained with 1% crystal violet (Solarbio, Beijing, China). Colony-formation numbers were counted under microscopy (Nikon, Tokyo, Japan).

Flow Cytometry

Cell apoptosis and cycle distribution were determined via flow cytometry. An annexin V–FITC apoptosis kit (Solarbio) was used for cell-apoptosis assays. SiHa and HeLa cells (10^5 cells/well) were added to 12-well plates and cultured for 48 hours. Subsequently, cells were harvested with trypsin and resuspended in the binding buffer, followed by incubation of 10 μL annexin V–FITC and propidium iodide (PI) for 10 minutes. Stained cells were measured with flow cytometry (Agilent, Hangzhou, China), and apoptotic rate was presented as the percentage of cells (Annexin V-$FITC^+$ and $PI^{-/+}$). For cell-cycle assays, SiHa and HeLa cells (2×10^5 cells/well) were placed in 12-well plates and cultured for 48 hours. Next, cells were collected, fixed via 70% ethanol (Sigma-Aldrich), and interacted with 50 μg/mL PI and RNase A for 20 minutes. Cell-cycle distribution was detected using flow cytometry.

Western Blot

Protein was isolated with RIPA lysis buffer (Thermo Fisher Scientific) and quantified with a BCA-assay kit (Sigma-Aldrich). Protein samples were subjected to SDS-PAGE and transfer of polyvinylidene fluoride membranes (Solarbio). The membranes were blocked in 5% nonfat milk, interacted with primary and secondary antibodies, and then incubated with ECL Western blotting substrate (Solarbio). GAPDH was regarded as a reference, and relative protein expression was normalized to the control group. Antibodies were provided by Abcam (Cambridge, UK): anti–cyclin D1 (ab226977, 1:5,000 dilution), anti-BCL2 (ab194583, 1:500 dilution), anti-PCNA (ab15497, 1:2,000 dilution), anti-LC3II/I (ab51520, 1:1,000 dilution), anti-ELK1 (ab131465, 1:500 dilution), anti-GAPDH (ab70699, 1:5,000 dilution), and horseradish peroxidase–conjugated IgG (ab6721, 1:10,000 dilution).

Dual Luciferase–Reporter Analysis, RNA Immunoprecipitation, and RNA Pull-Down

The complementary site between *circ_0000285* and *miR197-3p* was predicted using Circular RNA Interactome (https://circinteractome.nia.nih.gov) and that between *miR197-3p* and *ELK1* via starBase (http://star

base.sysu.edu.cn). Wild-type (WT) *circ_0000285* and WT *ELK1* were constructed by inserting the sequence of *circ_0000285* or *ELK1* 3′UTR containing *miR197-3p* binding sites into psiCheck-2 (Promega, Madison, WI, USA). Mutant (Mut) *circ_0000285* and Mut *ELK1* were generated via mutating the binding sites to CACCACU or ACCACU, respectively. WT or Mut luciferase-reporter vectors (600 ng) were transfected into SiHa and HeLa cells for luciferase-activity assays with a dual-luciferase assay system (Promega).

For RIP assays, the Magna RIP RNA-binding protein-immunoprecipitation kit (Sigma-Aldrich) was used. SiHa and HeLa cells (10^7 cells) were lysed in lysis buffer and interacted with magnetic beads coated with anti-Ago2 for 8 hours. Anti-IgG was used as NC. RNA on the beads was purified and abundance of *circ_0000285*, *miR197-3p*, and *ELK1* detected with qRT-PCR. For RNA pull-down assays, a magnetic RNA-protein pull-down kit (Thermo Fisher Scientific) was used. Biotinylated *miR197-3p* mimic (biotin-miR197-3p-WT), mutant (biotin-miR197-3p-Mut) and NC (biotin-miRNC) were formed with RiboBio (Guangzhou, China). SiHa and HeLa cells (10^7 cells) transfected with biotin-miR197-3p-WT, biotin-miR 197-3p-Mut, or biotin-miRNC were lysed and incubated with magnetic beads overnight. RNA on the beads was eluted and used for detection of *circ_0000285* levels via qRT-PCR.

Xenograft Model

BALB/c nude mice (5-week-old females) were obtained from Beijing Laboratory Animal Center (Beijing, China). The lentiviral vector of short-hairpin RNA for *circ_0000285* (sh-circ_0000285) or NC (sh-NC) was synthesized via RiboBio. HeLa cells were transfected with sh-circ_0000285 or sh-NC, and stably transfected cells were selected with puromycin. HeLa cells (5×10^6 cells/mouse) stably transfected with sh-circ_0000285 or sh-NC were subcutaneously inoculated into mouse flanks (n=5/group). Tumor volume was examined every week for 4 weeks and calculated as volume (mm^3) =length (mm) × width^2 (mm^2)/2. At the end of this experiment, mice were euthanized via cervical dislocation under isoflurane anesthesia. Tumor samples were weighed and then exploited for detection of *circ_0000285*, *miR197-3p*, and *ELK1* levels. Animal treatment met the standards of the *Guide for the Care and Use of Laboratory Animals* (People's Republic of China National Standard GB/T 35,-892–2018). Animal experiments were approved via the Animal Care and Use Committee of Zoucheng People's Hospital.

Statistical Analysis

GraphPad Prism 7 (GraphPad, La Jolla, CA, USA) was exploited for statistical analysis. Three independent experiments were conducted. Data are given as means ± SE. Differences were compared with Student's *t*-test or ANOVA, followed via Tukey's post hoc test as appropriate. Associations between circ_0000285 levels and clinical features of patients were analyzed with χ^2-tests. Statistical significance was regarded as $P<0.05$.

Results

circ_0000285 Expression Elevated in CC

To measure the level of *circ_0000285* in CC, we collected 30 paired cancer- and adjacent normal-tissue samples. qRT-PCR data revealed *circ_0000285* levels were evidently enhanced in CC tissue when compared to the normal group (Figure 1A). Patients were divided into high and low *circ_0000285*-expression groups according to the median value of *circ_0000285*. High expression of *circ_0000285* was associated with tumor size, differentiation, and International Federation of Gynecology and Obstetrics stage, but not with age or lymph-node metastasis (Table 1). *circ_0000285* levels were higher in CC cell lines (SiHa and HeLa) than normal cervical epithelial cells (H8, Figure 1B). To identify the circular structure of *circ_0000285*, RNA was treated with RNase R. Results showed that *circ_0000285* was more resistant to RNase R than linear *GAPDH* (Figure 1C and D). Meanwhile, with reverse transfection using random primers or oligo$(dT)_{18}$ primers, we found that *circ_0000285* did not have polyadenylation (Figure 1E and F). In addition, *circ_0000285* was mainly located in cytoplasm of SiHa and HeLa cells (Figure 1G and H). These data indicated that high expression of *circ_0000285* might have an important role in CC development.

circ_0000285 Knockdown Inhibits Viability, Colony Formation, Arrests Cell Cycle, and Induces Apoptosis and Autophagy in CC Cells

To explore the function of *circ_0000285* in CC development, loss-of-function experiments were performed in vitro by knockdown of *circ_0000285*. Efficacy >60% for *circ_0000285* knockdown using si-circ_0000285 was

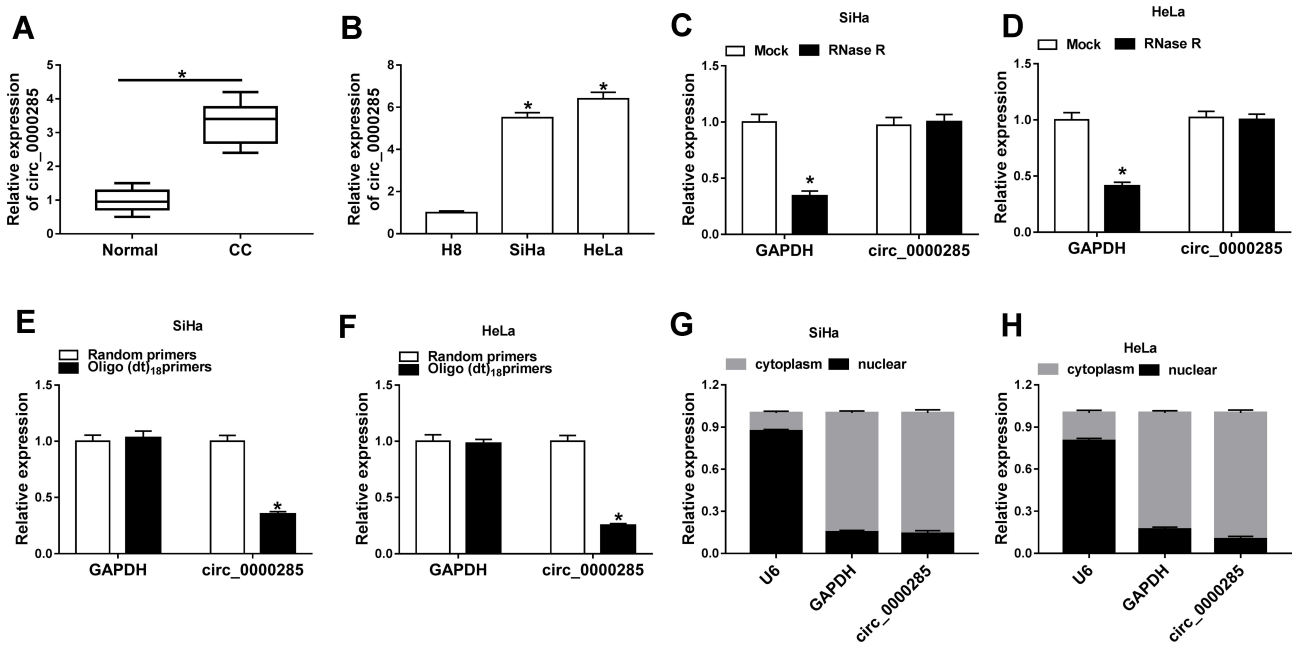

Figure 1 Expression of *circ_0000285* in CC. (**A**) *circ_0000285* expression CC andadjacent normal tissue via qRT-PCR (n=30). (**B**) *circ_0000285* levels in CC cells (SiHa and HeLa) and normal cervical epithelial cells (H8). (**C, D**) Levels of *circ_0000285* and *GAPDH* in SiHa and HeLa cells after treatment with RNase R. (**E, F**) Levels of *circ_0000285* and *GAPDH* after reverse transfection using random primers or oligo(dT)$_{18}$ primers. (**G, H**) Expression of *U6*, *GAPDH*, and *circ_0000285* cytoplasm and nuclear RNA. *P<0.05.

validated in SiHa and HeLa cells (Figure 2A). Meanwhile, si-circ_0000285 did not alter levels of *linear_0000285* (Figure 2B). MTT assays showed that *circ_0000285* knockdown obviously decreased the viability of SiHa and HeLa cells (Figure 2C). Moreover, analysis of flow cytometry showed that downregulation of *circ_0000285* promoted cell apoptosis and arrested the cell cycle at the G_0/G_1 phase (Figure 2D–F). Additionally, *circ_0000285* silence evidently suppressed the colony-formation ability of SiHa and HeLa cells (Figure 2G). Western blot assays showed that interference of *circ_0000285* markedly declined protein levels of PCNA, cyclin D1 and BCL2 and enhanced LC3-II/I levels in the two cell lines (Figure 2H). These results suggested that *circ_0000285* knockdown repressed CC development in vitro.

circ_0000285 is a Sponge for miR197-3p

Having got *circ_0000285* mainly located in cytoplasm, we wanted to explore whether *circ_0000285* could act as an miRNA sponge or ceRNA. Targets of *circ_0000285* were predicted via Circular RNA Interactome, which indicated that *miR197-3p* might be a potential target of *circ_0000285* (Figure 3A). To confirm the target association between *circ_0000285* and *miR197-3p*, we constructed WT circ_0000285 and Mut-circ_0000285. Dual luciferase–reporter assays showed that *miR197-3p* overexpression decreased luciferase activity >50%in the WT circ_0000285 group, but the suppressive effect was abolished in the Mut-circ_0000285 group (Figure 3B). Meanwhile, we explored the impact of *miR197-3p* on luciferase activity of nontargets (*circABCC2*, *circLRP6*, and *circSCAF11*). Results showed that *miR197-3p* did not affect the activity of nontargets (Figure 3C). Moreover, RNA pull-down and Ago2 RIP analyses displayed *circABCC2* bound with *miR197-3p* (Figure 3D and E). In addition, lower *miR197-3p* levels were found in CC tissue and cells than normal tissue and H8 cells, respectively (Figure 3F and G). Furthermore, the influence of *circ_0000285* on *miR197-3p* expression was assessed. The efficacy of *miR197-3p* inhibitor is validated in Figure 3H. *miR197-3p* level was elevated via silencing of *circ_0000285*, which was weakened via knockdown of *miR197-3p* (Figure 3I). These findings indicated that *circ_0000285* was a sponge for *miR197-3p* in CC cells.

miR197-3p Knockdown Reverses the Effect of circ_0000285 Silence on CC Development in vitro

Next, we explored whether *miR197-3p* was required for *circ_0000285*-mediated regulation of CC development. As displayed in Figure 4A and B, *miR197-3p* knockdown restored silence of *circ_0000285*-induced inhibition of

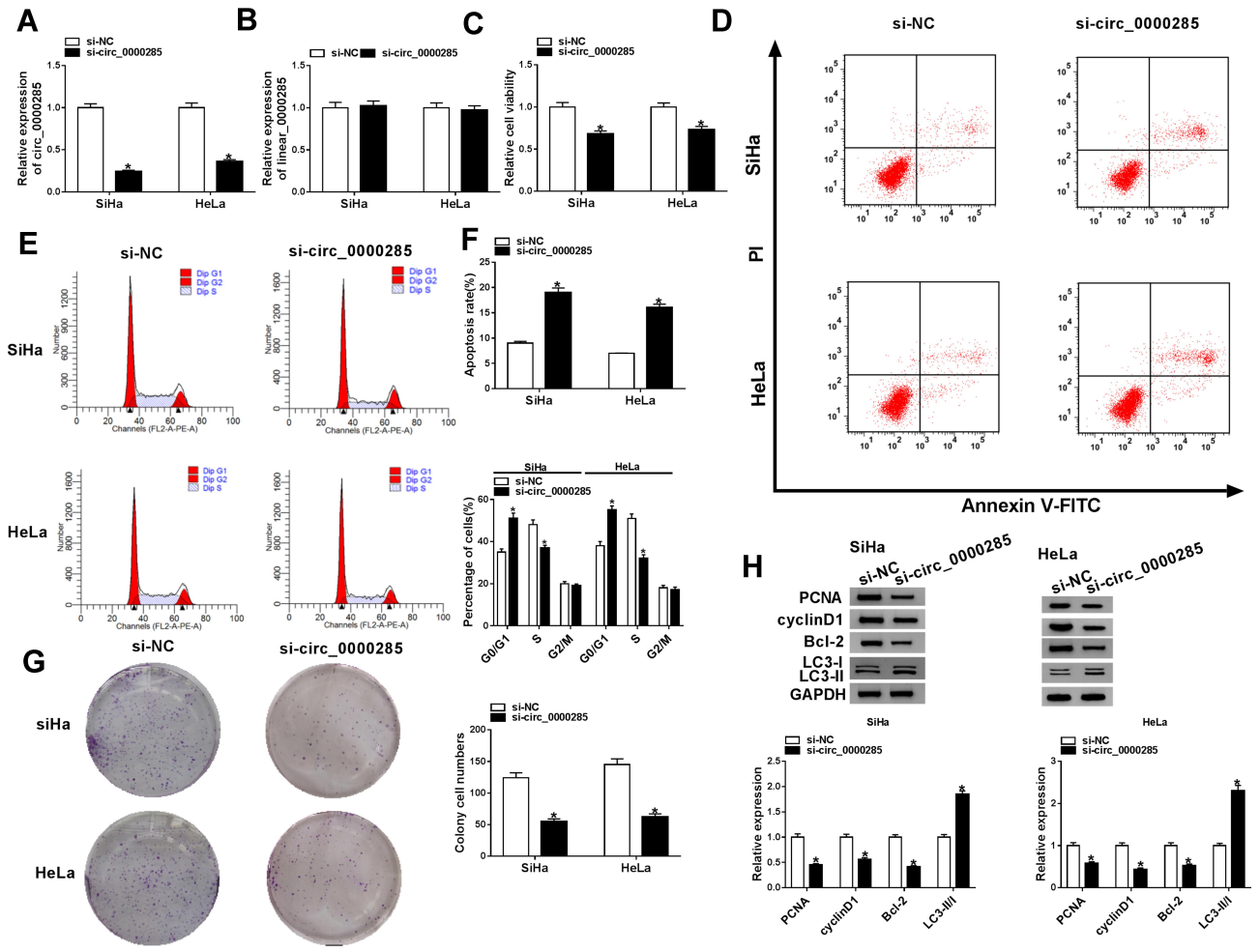

Figure 2 Effect of *circ_0000285* on CC-cell proliferation, apoptosis, cell cycle, colony formation, and autophagy. (**A, B**) The of *circ_0000285* and *linear_0000285* levels were measured in SiHa and HeLacells with transfection of si-circ_0000285 or si-NC. Cell viability (**C**), apoptosis and cell-cycle distribution(**D–F**), colony formation (**G**), and protein levels of PCNA, cyclin D1, BCL2 and LC3II/I (**H**) were detected in SiHa and HeLa cells with transfection of si-circ_0000285 or si-NC by MTT, flow cytometry, colony-formation assays and Western blot. *P<0.05.

cell viability and colony-formation ability in SiHa and HeLa cells. Furthermore, downregulation of *miR197-3p* weakened the knockdown of *circ_0000285*-induced G_0/G_1-phase arrest and cell apoptosis (Figure 4C–E). *miR197-3p* inhibition attenuated the regulatory effect of *circ_0000285* interference on protein levels of PCNA, cyclin D1, BCL2, and LC3-II/I in SiHa and HeLa cells (Figure 4F). These data indicated that *circ_0000285* knockdown suppressed CC development in vitro by increasing *miR197-3p*.

ELK1 is a Target of miR197-3p

To probe the ceRNA network further, targets of *miR197-3p* were searched. StarBase predicted *ELK1* as a candidate target of *miR197-3p*. To identify the target association between *miR197-3p* and *ELK1*, WT-ELK1 and Mut-ELK1 were constructed (Figure 5A). The influence of *circ_0000285* and *miR197-3p* on luciferase activity was analyzed. Transfection efficacy of the *circ_0000285*-overexpression vector is confirmed in Figure 5B. *miR197-3p* upregulation obviously decreased luciferase activity in the WT-ELK1 group, which was restored via upregulation of *circ_0000285*, while neither *circ_0000285* nor *miR197-3p* affected the activity in the Mut-ELK1 group (Figure 5C and D). In addition, Ago2 RIP assays showed that *miR197-3p* and *ELK1* were enriched in the same complex (Figure 5E). The Cancer Genome Atlas (TCGA) database showed that *ELK1* expression is enhanced in CC tissue (Figure 5F and G). Furthermore, the effect of *circ_0000285* and *miR197-3p* on ELK1 expression was investigated. Transfection efficacy of pc-ELK1 is validated in Figure 5H. As shown in Figure 5I, ELK1-protein levels were evidently reduced via *miR197-3p* overexpression and restored via introduction of pc-ELK1. *circ_0000285* knockdown significantly decreased ELK1-

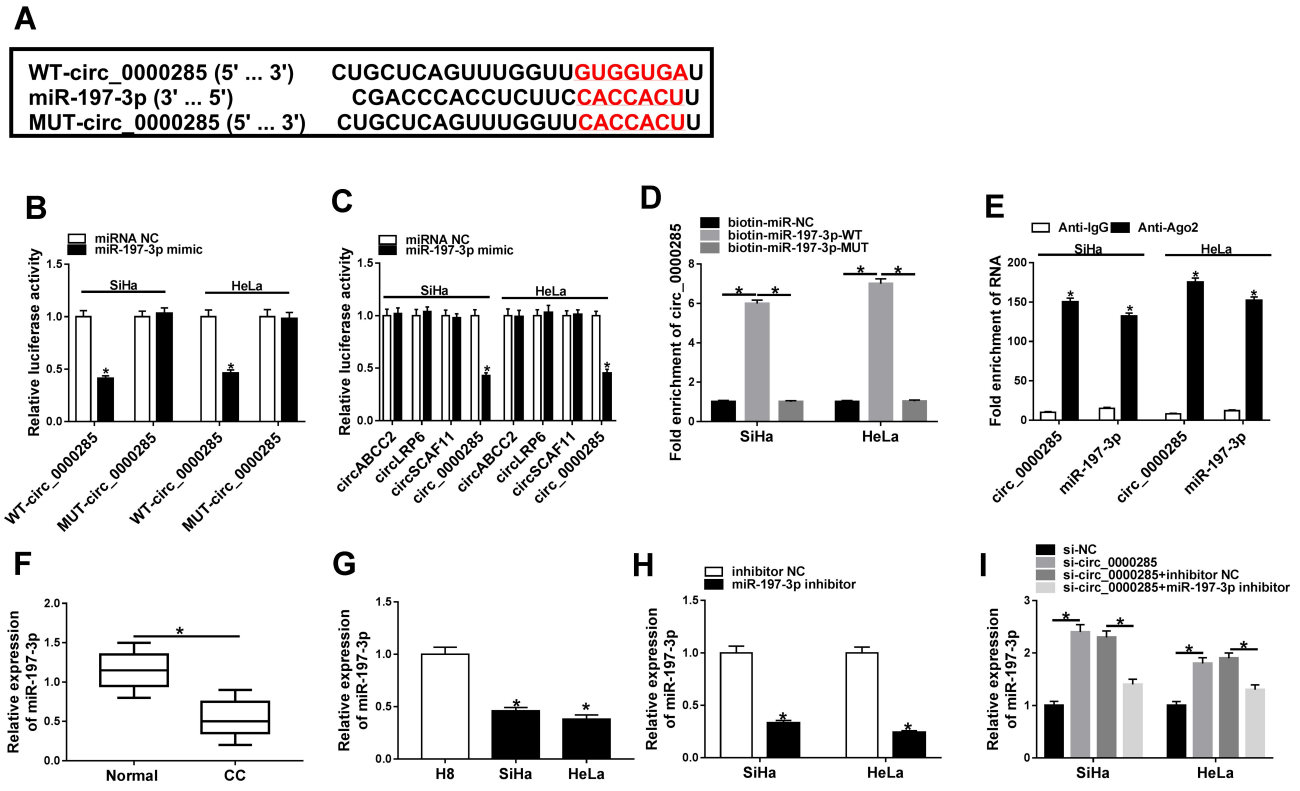

Figure 3 The association between *circ_0000285* and *miR197-3p*. (**A**) Circular RNA Interactome tool searched the binding sites of *circ_0000285* and *miR-197-3p*. (**B**) Luciferase activity was detected in cells co-transfected with WT-circ_0000285 or mut-circ_0000285 and miR197-3p mimic or miRNA NC. (**C**) Luciferaseactivity in cells cotransfected with WT circ_0000285 or other circRNAs withoutbinding sites and *miR197-3p* mimic or miRNA NC. (**D**) *circ_0000285* levels after RNApull-down. (**E**) *circ_0000285* and *miR197-3p* levels after Ago2 RIP. (**F**) *miR197-3p* level in CC and adjacent normal tissue via qRT-PCR. n=30. (**G**) *miR197-3p* abundancein CC and H8 cells. (**H**) *miR197-3p* expression in SiHa and HeLa cells with transfection of *miR197-3p* inhibitor or inhibitor NC. (**I**) *miR197-3p* abundance in SiHa and HeLa cells transfected with si-NC, si-circ_0000285, and si-circ_0000285 + inhibitor NC or *miR197-3p* inhibitor. *P<0.05.

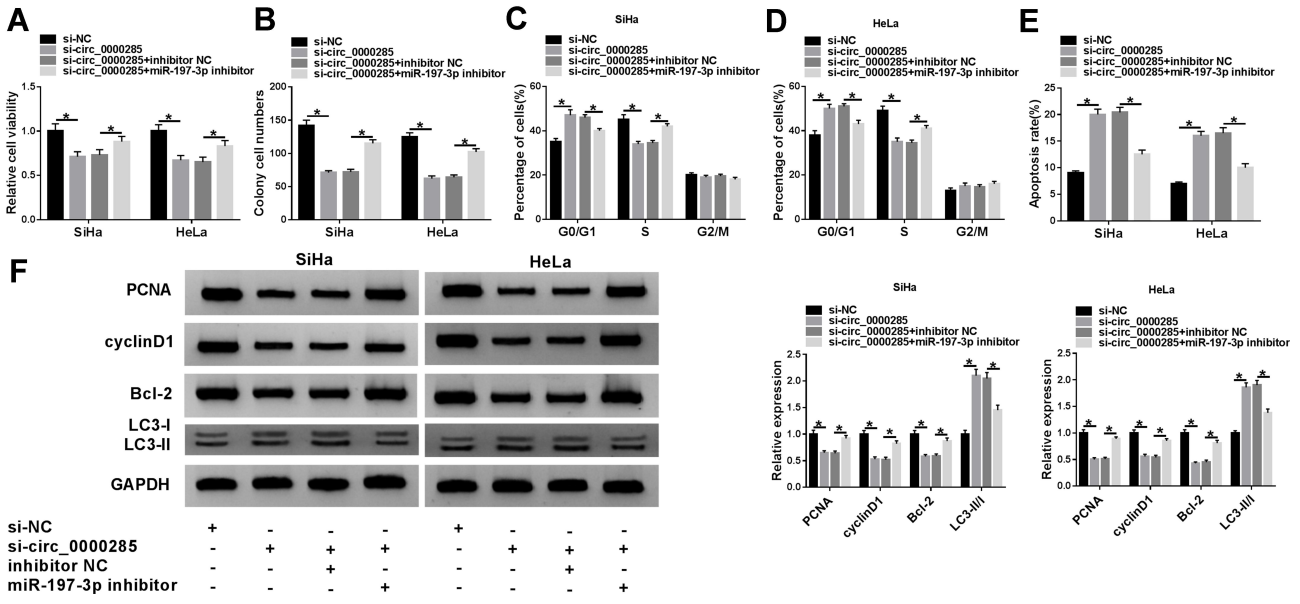

Figure 4 The effect of *miR197-3p* on *circ_0000285*-mediated CC-cell proliferation, apoptosis, cell cycle, colony formation, and autophagy. Cell viability (**A**), colony formation (**B**), cell-cycle distribution (**C, D**), apoptosis (**E**), and protein levels of PCNA, cyclin D1, BCL2, and LC3II/I (**F**) in SiHa and Hela cells with of si-NC, si-circ_0000285, si-circ_0000285 + inhibitor NC, or *miR197-3p* inhibitor. *P<0.05.

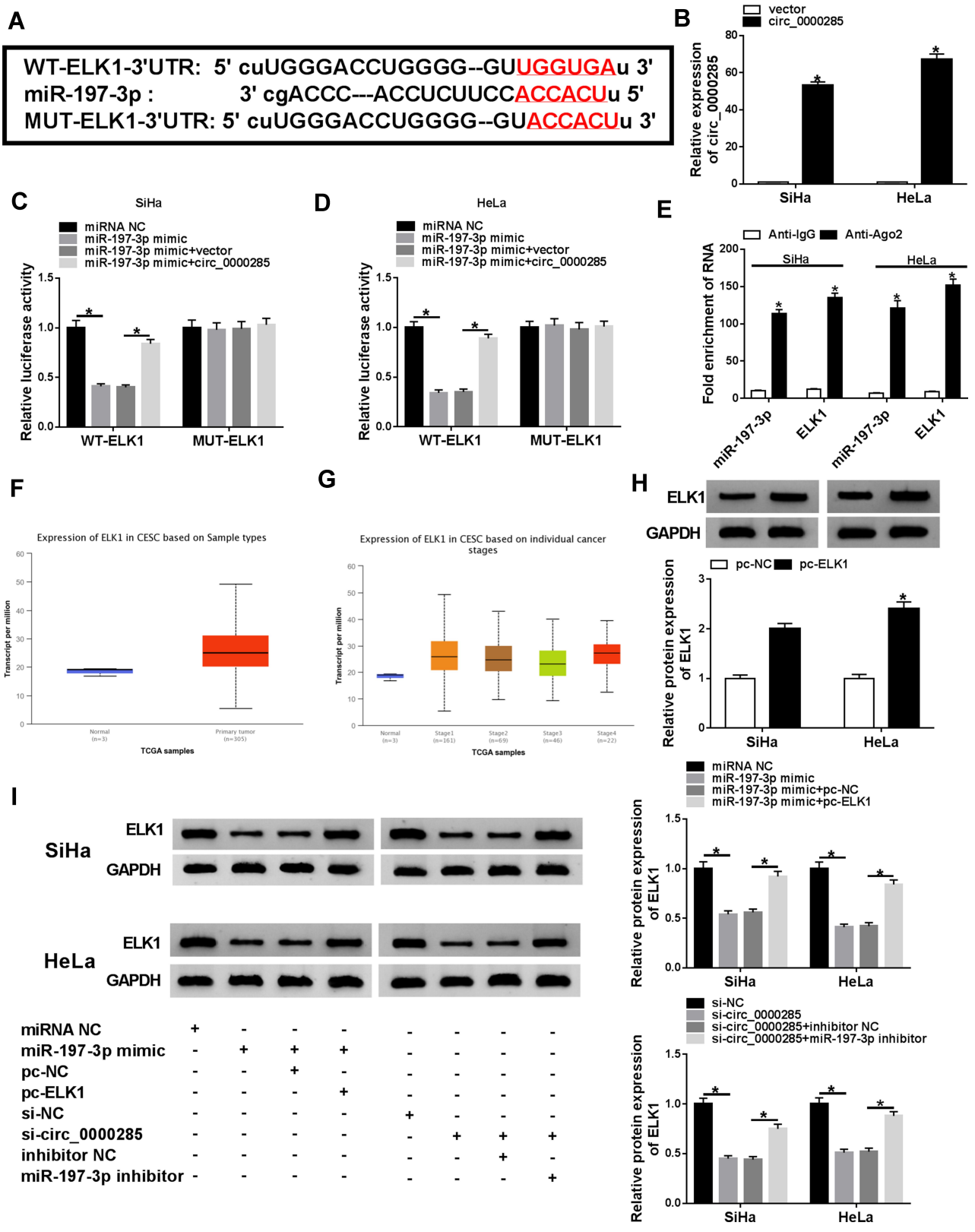

Figure 5 The association between *miR197-3p* and *ELK1*. (**A**) The complementary sequence of *miR197-3p* and *ELK1* was predicted via StarBase. (**B**) *circ_0000285* expression was detected in SiHa andHeLa cells transfected with *circ_0000285* overexpression vector or control vector. (**C, D**) Luciferase activity was detected in cells co-transfected with WT ELK1, mut-ELK1 and miRNA NC, *miR197-3p* mimic, *miR197-3p* mimic + vector, or *circ_0000285*-overexpression vector. (**E**) *ELK1* and *miR197-3p* levels after Ago2 RIP. (**F, G**) *ELK1* expression in CC tissue predicted via TCGAdatabase. (**H**) ELK1 protein levels in SiHa and HeLa cells transfected with pc-ELK1 or pc-NC by Western blot. (**I**) ELK1-protein abundance in SiHa and HeLa cells transfected with miRNA NC, *miR197-3p* mimic, *miR197-3p* mimic + pc-ELK1, *miR197-3p* mimic + pc-NC, si-NC, si-circ_0000285, si-circ_0000285 + inhibitor NC, or *miR197-3p* inhibitor. *P<0.05.

protein expression, and this effect was weakened via down-regulation of *miR197-3p*. These data indicate that *ELK1*, as a target of *miR197-3p*, was regulated via *circ_0000285* through competitively binding with *miR197-3p*.

miR197-3p Overexpression Represses Viability and Colony Formation, Arrests Cell Cycle, and Facilitates Apoptosis and Autophagy via Targeting ELK1 in CC Cells

To explore how and whether *miR197-3p* took part in CC development in vitro, SiHa and HeLa cells were transfected with miRNA NC, *miR197-3p* mimic, *miR197-3p* mimic + pc-NC, or pc-ELK1. Overexpression of *miR197-3p* remarkably inhibited cell viability and colony formation (Figure 6A and B), induced cell-cycle arrest at the G_0/G_1 phase (Figure 6C and D), promoted cell apoptosis (Figure 6E), decreased protein levels of PCNA, cyclin D1, and BCL2, and increased LC3-II/I levels (Figure 6F and G) in SiHa and HeLa cells. These events were alleviated via ELK1 upregulation (Figure 6A–G). These findings suggested that *miR197-3p* repressed CC development by targeting *ELK1* in vitro.

Knockdown of circ_0000285 Reduces Xenograft Tumor Growth In Vivo

To explore the role of *circ_0000285* in CC development in vivo, HeLa cells stably transfected with sh-circ_0000285 or sh-NC were used to establish a xenograft model, and were classified as sh-circ_0000285 or sh-NC (n=5). Tumor volume was examined every week and tumor weight measured at the end point. As shown in Figure 7A and B, tumor volume and weight were evidently reduced in the sh-circ_0000285 group in comparison to the sh-NC group. Furthermore, expression levels of *circ_0000285*, *miR197-3p* and *ELK1* were examined in each group at the end point. As displayed in Figure 7C–F, *circ_0000285* and *ELK1* levels were markedly decreased and *miR197-3p* expression enhanced in the sh-circ_0000285 group in comparison to the sh-NC group.

Discussion

CC is a global public health problem in women.[26] circRNAs can be used as important biomarkers for the development and treatment of CC.[8] In this work, *circ_0000285* was upregulated in CC, consistent with a previous study.[14] This indicated that high expression of *circ_0000285* might be associated with CC malignancy. Our study confirmed that *circ_0000285* knockdown suppressed CC development in vitro and in vivo. Moreover, here we are the first to identify the potential ceRNA network of *circ_0000285–miR197-3p–ELK1* in CC.

Previous research has suggested that *circ_0000285* knockdown repressed CC-cell proliferation via decreasing cell viability and arresting the cell cycle at the G_0/G_1 phase.[14] These results were also confirmed in our study.

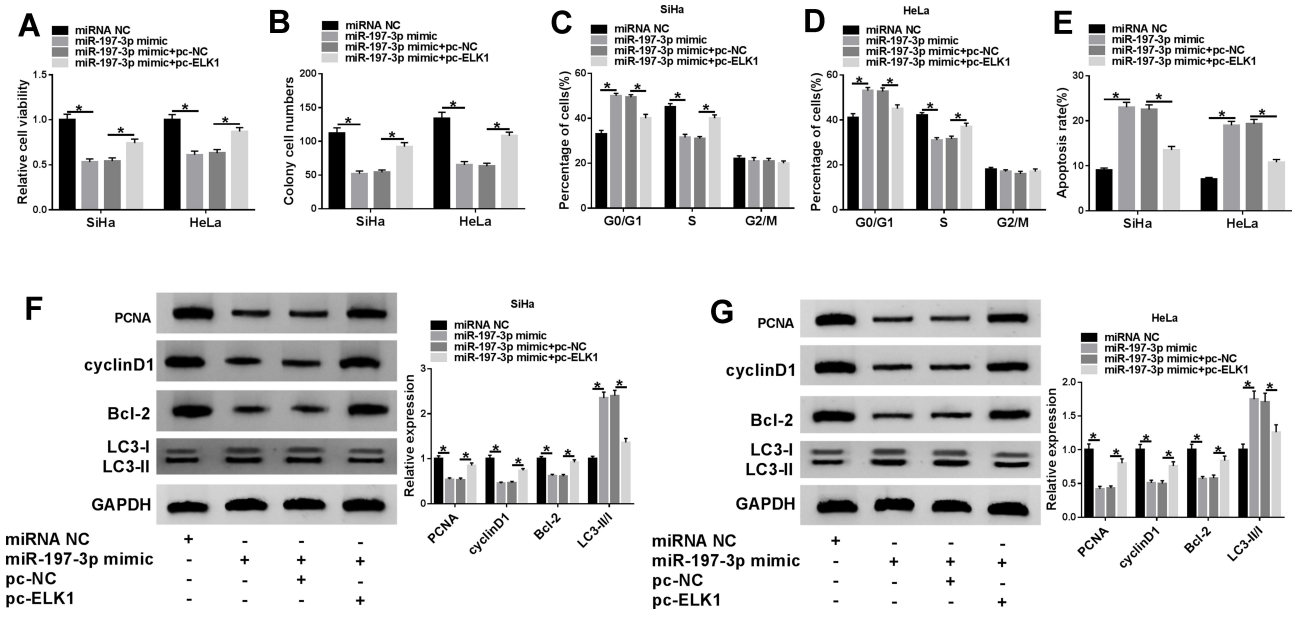

Figure 6 Effect of *miR197-3p* and *ELK1* on CC-cell proliferation, apoptosis, cell cycle, colonyformation and autophagy. Cell viability (**A**), colony formation (**B**), cell-cycle distribution (**C, D**), apoptosis (**E**), and protein levels of PCNA, cyclin D1, BCL2, and LC3II/I (**F, G**) were detected in SiHa and HeLa cellstransfected with miRNA NC, *miR197-3p* mimic, *miR197-3p* mimic + pc-ELK1, or pc-NC. *$P<0.05$.

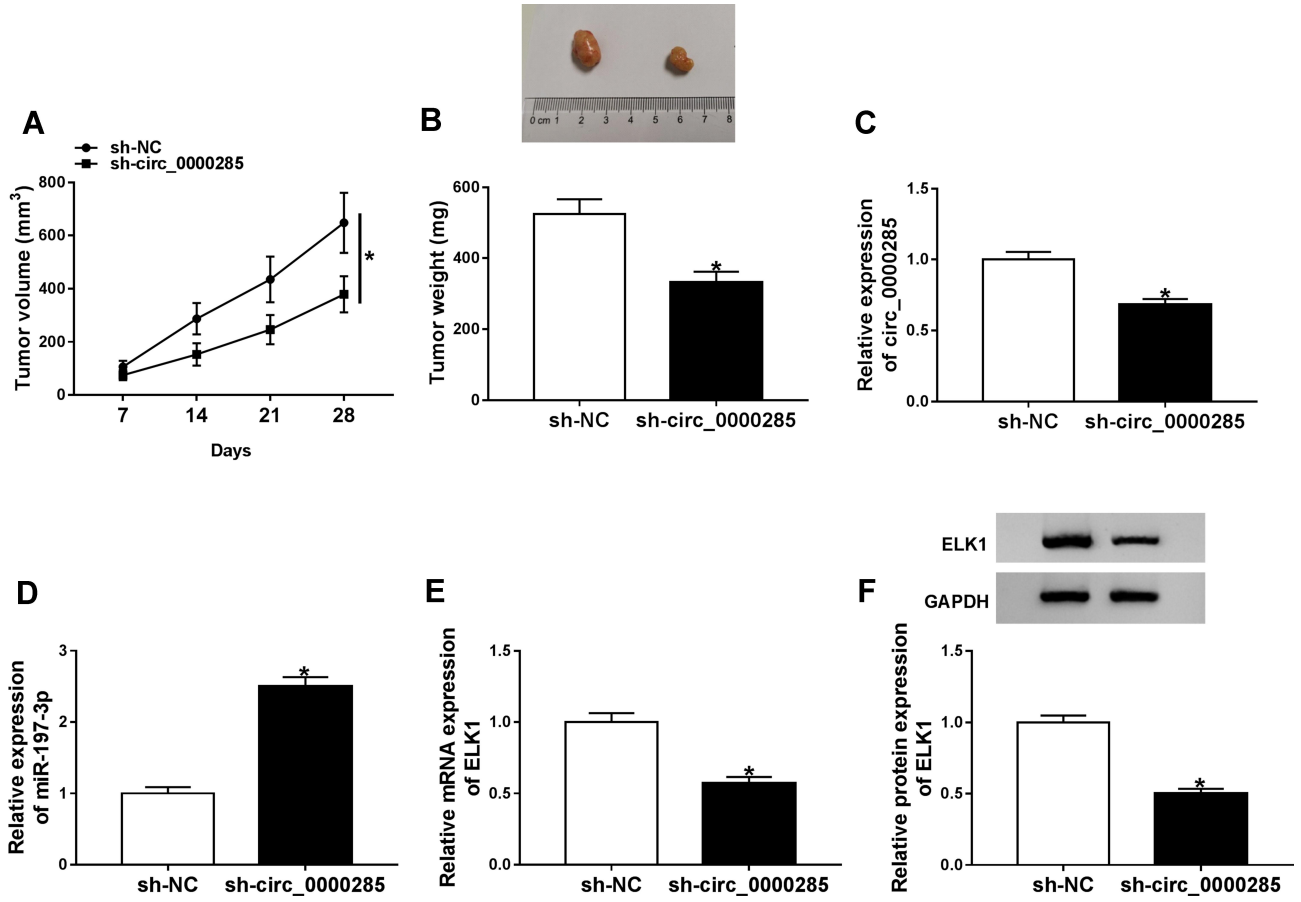

Figure 7 Effect of *circ_0000285* on xenograft tumor growth. (**A**) Tumor volume was monitored every week. (**B**) Tumor weight measured at the end point. (**C–F**) The levels of *circ_0000285*, *miR197-3p*, and *ELK1* mRNA and protein in tumor tissue in each group. *$P<0.05$.

Moreover, colony formation, apoptosis, and autophagy were also related to cell growth and malignancy in CC.[27,28] By performing related experiments and detecting related biomarkers,[27,30] we found that *circ_0000285* silence inhibited CC-cell growth by reducing colony formation and promoting apoptosis and autophagy. These data implied the carcinogenic role of *circ_0000285* in CC, which was also in agreement with that in other cancers.[10,12,13] Nevertheless, the mechanism addressed via *circ_0000285* in CC development needs more exploration.

The ceRNA network is an important mechanism underlying the role of circRNA located at cytoplasm in cancers.[31] A study has indicated *circ_0000285* can function as a ceRNA for *miR599* to regulate $TGF\beta_2$.[12] Our study is the first to confirm *circ_0000285* is a sponge for *miR197-3p* via dual luciferase–reporter assays, RIP, and RNA pull-down. In this research, downregulated *miR197-3p* was measured in CC, consistent with former work.[18] That paper showed that *miR197-3p* had a tumor-suppressive role in CC by suppressing proliferation and invasion.[18] Similarly, our research also identified the antitumor effect of *miR197-3p* in CC via regulating cell viability, colony formation, the cell cycle, apoptosis, and autophagy. However, this function iss opposite to that in some cancers, such as thyroid cancer and bladder cancer.[16,32] We hypothesized this might result from altered tumor microenvironments in different cancers. Furthermore, the rescue experiments indicated that *circ_0000285* regulated CC development via sponging *miR197-3p*.

To analyze ceRNA cross talk further, we explored and analyzed targets of *miR197-3p*. Previous studies have validated multiple targets of *miR197-3p* in different cancers, such as *FoxM1*, *KLF10*, and *PKCβ*.[18,32,33] In this research, we were the first to identify *miR197-3p* directly targeting *ELK1*, an oncogene in CC predicted via the TCGA. Former work has indicated that *ELK1* can promote CC development via inducing proliferation, migration, and invasion and inhibiting apoptosis and autophagy.[24,34] Similarly, this study also uncovered the oncogenic role of

ELK1 in CC cells by reversing the anticancer role of *miR197-3p*. This also indicated that *miR197-3p* regulated CC development via directly targeting *ELK1*. In addition, through dual luciferase–reporter assays and Western blot, we found that *circ_0000285* modulated *ELK1* expression by competitively binding with *miR197-3p*, implying the ceRNA network of *circ_0000285–miR197-3p–ELK1* in CC in vitro. Also, we identified the anticancer role of *circ_0000285* knockdown in CC in vivo using a murine xenograft model, also in agreement with a previous study.[14] *miR197-3p* and *ELK1* were dysregulated in xenograft tumor tissue, indicating that *miR197-3p* and *ELK1* might also explain *circ_0000285* function in vivo.

In conclusion, *circ_0000285* silence inhibited CC development, possibly via regulating *miR197-3p* and *ELK1* in a ceRNA-based mechanism. This study indicates a new mechanism for understanding the pathogenesis of CC and suggests that *circ_0000285* might be a target for the treatment of CC.

Disclosure

The authors report no funding and no conflicts of interest in this work.

References

1. Cohen PA, Jhingran A, Oaknin A, et al. Cervical cancer. *Lancet*. 2019;393(10167):169–182. doi:10.1016/S0140-6736(18)32470-X
2. Torre LA, Siegel RL, Ward EM, et al. Global cancer incidence and mortality rates and trends--an update. *Cancer Epidemiol Biomarkers Prev*. 2016;25(1):16–27. doi:10.1158/1055-9965.EPI-15-0578
3. Johnson CA, James D, Marzan A, et al. Cervical cancer: an overview of pathophysiology and management. *Semin Oncol Nurs*. 2019;35(2):166–174. doi:10.1016/j.soncn.2019.02.003
4. Huang J, Zhou Q, Li Y. Circular RNAs in gynecological disease: promising biomarkers and diagnostic targets. *Biosci Rep*. 2019;39(5):BSR20181641. doi:10.1042/BSR20181641
5. Kristensen LS, Andersen MS, Stagsted LVW, et al. The biogenesis, biology and characterization of circular RNAs. *Nat Rev Genet*. 2019;20(11):675–691. doi:10.1038/s41576-019-0158-7
6. Ng WL, Mohd Mohidin TB, Shukla K. Functional role of circular RNAs in cancer development and progression. *RNA Biol*. 2018;15(8):995–1005. doi:10.1080/15476286.2018.1486659
7. Tay Y, Rinn J, Pandolfi PP. The multilayered complexity of ceRNA crosstalk and competition. *Nature*. 2014;505(7483):344–352. doi:10.1038/nature12986
8. Chaichian S, Shafabakhsh R, Mirhashemi SM, et al. Circular RNAs: a novel biomarker for cervical cancer. *J Cell Physiol*. 2020;235(2):718–724. doi:10.1002/jcp.29009
9. Varghese VK, Shukla V, Kabekkodu SP, et al. DNA methylation regulated microRNAs in human cervical cancer. *Mol Carcinog*. 2018;16(5):370–382. doi:10.1002/mc.22761
10. Shuai M, Hong J, Huang D, et al. Upregulation of circRNA_0000285 serves as a prognostic biomarker for nasopharyngeal carcinoma and is involved in radiosensitivity. *Oncol Lett*. 2018;16(5):6495–6501. doi:10.3892/ol.2018.9471
11. Chi BJ, Zhao DM, Liu L, et al. Downregulation of hsa_circ_0000285 serves as a prognostic biomarker for bladder cancer and is involved in cisplatin resistance. *Neoplasma*. 2019;66(2):197–202. doi:10.4149/neo_2018_180318N185
12. Zhang Z, Pu F, Wang B, et al. Hsa_circ_0000285 functions as a competitive endogenous RNA to promote osteosarcoma progression by sponging hsa-miRNA-599. *Gene Ther*. 2019:1–10.
13. Qin J-B, Chang W, Yuan G-H, et al. Circular RNA hsa_circ_0000285 acts as an oncogene in laryngocarcinoma by inducing Wnt/beta-catenin signaling pathway. *Eur Rev Med Pharmacol Sci*. 2019;23(24):10803–10809. doi:10.26355/eurrev_201912_19783
14. Chen RX, Liu HL, Yang LL, et al. Circular RNA circRNA_0000285 promotes cervical cancer development by regulating FUS. *Eur Rev Med Pharmacol Sci*. 2019;23(20):8771–8778. doi:10.26355/eurrev_201910_19271
15. Nahand JS, Taghizadeh-Boroujeni S, Karimzadeh M, et al. microRNAs: new prognostic, diagnostic, and therapeutic biomarkers in cervical cancer. *J Cell Physiol*. 2019;234(10):17064–17099. doi:10.1002/jcp.28457
16. Liu K, Huang W, Yan D-Q, et al. Overexpression of long intergenic noncoding RNA LINC00312 inhibits the invasion and migration of thyroid cancer cells by down-regulating microRNA-197-3p. *Biosci Rep*. 2017;37(4):BSR20170109. doi:10.1042/BSR20170109
17. Ni JS, Zheng H, Huang ZP, et al. MicroRNA-197-3p acts as a prognostic marker and inhibits cell invasion in hepatocellular carcinoma. *Oncol Lett*. 2019;17(2):2317–2327. doi:10.3892/ol.2018.9848
18. Hu Q, Du K, Mao X, et al. miR-197 is downregulated in cervical carcinogenesis and suppresses cell proliferation and invasion through targeting forkhead box M1. *Oncol Lett*. 2018;15(6):10063–10069. doi:10.3892/ol.2018.8565
19. Ahmad A, Zhang W, Wu M, et al. Tumor-suppressive miRNA-135a inhibits breast cancer cell proliferation by targeting ELK1 and ELK3 oncogenes. *Genes Genomics*. 2018;40(3):243–251. doi:10.1007/s13258-017-0624-6
20. Kong Y, Yin J, Fu Y, et al. Suppression of Elk1 inhibits thyroid cancer progression by mediating PTEN expression. *Oncol Rep*. 2018;40(3):1769–1776. doi:10.3892/or.2018.6554
21. Fan H-X, Feng Y-J, Zhao X-P, et al. MiR-185-5p suppresses HBV gene expression by targeting ELK1 in hepatoma carcinoma cells. *Life Sci*. 2018;213:9–17. doi:10.1016/j.lfs.2018.10.016
22. Fan C, Lin B, Huang Z, et al. MicroRNA-873 inhibits colorectal cancer metastasis by targeting ELK1 and STRN4. *Oncotarget*. 2019;10(41):4192–4204. doi:10.18632/oncotarget.24115
23. Zhao H, Hu G-M, Wang W-L, et al. LncRNA TDRG1 functions as an oncogene in cervical cancer through sponging miR-330-5p to modulate ELK1 expression. *Eur Rev Med Pharmacol Sci*. 2019;23(17):7295–7306. doi:10.26355/eurrev_201909_18834
24. Tang Q, Chen Z, Zhao L. Circular RNA hsa_circ_0000515 acts as a miR-326 sponge to promote cervical cancer progression through up-regulation of ELK1. *Aging*. 2019;11(22):9982–9999. doi:10.18632/aging.102356
25. Livak KJ, Schmittgen TD. Analysis of relative gene expression data using real-time quantitative PCR and the 2−ΔΔCT method. *Methods*. 2001;25(4):402–408. doi:10.1006/meth.2001.1262
26. Small W Jr, Bacon MA, Bajaj A, et al. Cervical cancer: a global health crisis. *Cancer*. 2017;123(13):2404–2412. doi:10.1002/cncr.30667
27. Gao J, Yu H, Guo W, et al. The anticancer effects of ferulic acid is associated with induction of cell cycle arrest and autophagy in cervical cancer cells. *Cancer Cell Int*. 2018;18(1):102. doi:10.1186/s12935-018-0595-y
28. Huang S, Xie T, Liu W. Icariin inhibits the growth of human cervical cancer cells by inducing apoptosis and autophagy by targeting mTOR/PI3K/AKT signalling pathway. *J BUON*. 2019;24(3):990–996.
29. Wang S-C. PCNA: a silent housekeeper or a potential therapeutic target? *Trends Pharmacol Sci*. 2014;35(4):178–186. doi:10.1016/j.tips.2014.02.004
30. Lu H-J, Jin P-Y, Tang Y, et al. microRNA-136 inhibits proliferation and promotes apoptosis and radiosensitivity of cervical carcinoma through the NF-κB pathway by targeting E2F1. *Life Sci*. 2018;199:167–178. doi:10.1016/j.lfs.2018.02.016

31. Thomson DW, Dinger ME. Endogenous microRNA sponges: evidence and controversy. *Nat Rev Genet*. 2016;17(5):272–283. doi:10.1038/nrg.2016.20
32. Li Z, Hong S, Liu Z. LncRNA LINC00641 predicts prognosis and inhibits bladder cancer progression through miR-197-3p/KLF10/PTEN/PI3K/AKT cascade. *Biochem Biophys Res Commun*. 2018;503(3):1825–1829. doi:10.1016/j.bbrc.2018.07.120
33. Chen Z, Ju H, Zhao T, et al. hsa_circ_0092306 targeting miR-197-3p promotes gastric cancer development by regulating PRKCB in MKN-45 cells. *Mol Ther Nucleic Acids*. 2019;18:617–626. doi:10.1016/j.omtn.2019.08.012
34. Zhang P, Kong F, Deng X, et al. MicroRNA-326 suppresses the proliferation, migration and invasion of cervical cancer cells by targeting ELK1. *Oncol Lett*. 2017;13(5):2949–2956. doi:10.3892/ol.2017.5852